Department of the Navy
Office of Naval Research
Fluid Mechanics Branch
Contract N6onr-244 Task Order II
NR 062-010

AN EXPERIMENTAL STUDY OF AXIAL FLOW PUMP CAVITATION

P. Guinard
T. Fuller
A. J. Acosta

Hydrodynamics Laboratory
California Institute of Technology
Pasadena, California

Project Supervisor
A. J. Acosta

Approved by:
A. Hollander

Report No. E-19.3
August 1953

CONTENTS

ABSTRACT

A qualitative study of the effects of cavitation on the performance of an axial flow pump was made. Photographic evidence shows that cavitation need not occur first on the blade surface but could occur in the free stream. This phenomenon is ascribed to a flow through the tip clearance space. Cavitation similarity was found to be determined by the cavitation number K, Thoma's σ, or the suction specific speed S for the conditions of these tests.

INTRODUCTION

Axial flow pumps characteristically operate with low submergence and high speed so that the pump is either cavitating or is on the verge of it. The transition between the critical stages of cavitation and the final stages in which gross changes in flow and performance take place is, for the most part, a gradual one, and for various applications both of these conditions are of importance. For use in pumping installations the question of limitation of submergence and reduction of efficiency are of greatest concern, whereas for the application of axial flow pumps in pumpjet propulsion systems, one of the major problems is the prevention of cavitation and cavitation damage.

It is usually assumed that as long as the extent of cavitation is small the usual affinity laws may be used for modeling between similar pumps of different sizes and speeds. However, according to Tenot[1*] a different similitude law must be used when the cavitation is in the range between incipient and a "critical" condition defined by a sharp break in the performance curve. In view of the rather limited information available concerning the detailed and over-all behavior of cavitating turbomachines, it is important to ascertain the validity of such modeling criteria for cavitation flows and to make visual observations of the internal flow correlated wherever possible with the over-all flow behavior.

---

*See references on page 10.

EXPERIMENTAL WORK

Description of Tests

Over-all performance cavitation tests of axial flow pumps are common, and it is the structure of the internal flow about which least is known, hence the major emphasis in this work is directed towards obtaining at least qualitative photographic records of cavitation phenomena over various operating conditions of the pump. Torque, speed, head and flow rate through the pump were also measured for various cavitating conditions and also with no cavitation so that performance changes could be detected. Data and photographs of the inception of cavitation were also taken for various operating conditions.

Test Setup

An 8-in. Peerless axial flow pump was used in the tests. Since the basic laboratory facilities are described in Refs. 2 and 3, no great elaboration of their details will be given here. Briefly, however, the test stand is provided with a 30 hp, 1800 rpm d-c motor mounted as a vertical dynamometer which may be controlled from 200 to 2,000 rpm. A service pump, sump, and suitable system of piping are available to meter and deliver up to 4 cfs of water at pressures ranging from about 30 psi to 15 in. Hg vacuum. Figure 1 is a photograph of the test floor, the dynamometer and pump test setup being shown schematically in Fig. 2.

In order to make the flow visible, the section of the pump bowl unit enclosing the impeller was removed and replaced with a square lucite block bored out to give a 0.010-in. radial tip clearance and left with flat faces to minimize optical distortion. The pump was driven by a dynamometer through two universal joints in order to obviate misalignment problems, and the lower motor bearing absorbed all pump thrust. Since the pump unit was not sufficiently rigid to withstand the lateral pressure reactions from the suction and discharge pipes, the whole unit was suspended from one point so that there would be no bending of the pump drive line.

Measurements and Instrumentation

As mentioned before, the over-all quantities measured were torque, speed, flow rate and head. Head was determined by measuring the static

pressure rise between the pump suction pipe line and discharge line, which are of the same size. A honeycomb flow straightener was installed in the suction line and a vane elbow was used with thirteen blades for the 90^{o} turn. Flow profile measurements before and after the two elbows were made in addition to loss measurements (Ref. 3), so that the performance of the bowl itself could be determined, i.e., the elbow losses were not charged to the pump. Torque was measured by loading an arm fastened to the motor body with pan weights hung from a pulley. Indicator lights set 0.004 in. apart could be used for rough balance, while for fine balance a Statham strain gage and galvanometer were used to determine the null position. Under noncavitating conditions the force on the torque arm was repeatable to about 3 grams out of 1,000.

Differential mercury manometers graduated in 0.001 ft were used to measure the head and also the static pressure in the plane of the impeller.

Photographs of the impeller were taken with a 4 x 5 view camera in conjunction with an Edgerton type single flash lamp triggered by a commutator on the motor shaft.

Procedure and Results

Noncavitating performance was determined over a range of flow rates varying from about 25 to 113 percent of the "normal" or best efficiency flow rate and is presented in Fig. 3 in terms of efficiency, dimensionless head coefficient ψ, torque coefficient τ, and dimensionless flow rate coefficient φ (see "notation"). For the cavitating runs an arbitrary suction pressure at the impeller was established and the performance determined over the complete head-flow rate diagram. These data are presented in Figs. 4 and 5 as variations in the torque and head, respectively, at constant flow rate for various inlet pressure conditions vs. Thoma's cavitation similarity parameter sigma (σ).

Some difficulty was experienced in obtaining reproducible torque readings. Due to the flexibility of the pump assembly, variations of system pressure caused, in spite of the precautions taken, slight binding of the drive shaft. By maintaining a constant suction pressure, torque changes due to system pressure were minimized and for this reason all performance runs were taken in the manner described. In order to determine the impeller and

bowl performance alone, the bearing and windage torques were not included in the performance calculations. They were measured by running the pump at a very low speed (50 rpm). For the reasons mentioned above, the torque readings should not be given undue weight, however the general behavior of torque with σ should be correct.

Runs were taken at rotative speeds of 800, 1000, 1400 and 1700 rpm. However, the data at the last two speeds are the most reliable because of the resulting greater forces and pressures involved.

DISCUSSION

Over-all Characteristics

The performance characteristics are given in Fig. 3 for nominal non-cavitating conditions and they are typical of commercial axial flow pumps, although even with the elbow losses not accounted for the efficiency seems somewhat high. The dimensionless flow rate $\varphi = 0.171$ was chosen as the normal or design point since it is the point of best efficiency. At this flow rate, the angle of attack to the blade chord is $1\text{-}1/2^{\circ}$ and the specific speed is 12,700 (based on gpm).

Cavitation Characteristics

A plot of developed head vs. σ is given in Fig. 5 for various values of the flow rate coefficient. At the best efficiency point it was not possible with the range of parameters available to cause a significant change in the developed head, even though substantial cavitation on the blades was present at the lowest value of σ. However, for reduced flow rates the head first increases as the inlet pressure (or σ) is reduced and then drops off rather sharply. This behavior is not uncommon for centrifugal pumps at reduced flow rates, and is also typical of axial flow machines.[4] A common and useful parameter for cavitation performance is the suction specific speed S (see "notation"). This parameter is also plotted in Fig. 5 for the design flow rate. At the design point, a suction specific speed of 5,000 may be obtained without loss in head although due to an increase in torque the efficiency has dropped. This value is considerably below the "safe" limit given by the Hydraulic Institute for performance of such pumps, i. e.,

$S \leq 8,140$. However, operation of the pump at slightly above the design condition (115% Q_n) and at σ of 2.76 would result in this limiting value, so in all probability the pump tested is representative of commercial design. It should be pointed out that for centrifugal pumps, as the flow rate is reduced, less absolute suction pressure is required for the suppression of cavitation, whereas for axial flow pumps the reverse situation occurs.

The shaded areas of Figs. 4 and 5 represent the region in which the inception of cavitation may occur. This region is also presented in Fig. 6 as values of the incipient cavitation parameter K vs. percent design flow rate. The cavitation number K is defined by the ratio of the static pressure above the vapor pressure to the inlet relative velocity head, rather than on the vector mean of the inlet and outlet velocities as is sometimes used. Since the axial component of this velocity is small, variation in K is substantially equivalent to variation in the static pressure. It is seen that two curves are given, one for the appearance of cavitation with decreasing static pressure and one for increasing pressure. Such a "hysteresis" effect is typical for cavitation flows[5] although it depends somewhat upon dissolved air content and the rapidity with which the pressure is changed. It should also be noted from Fig. 6 that cavitation inception on rotating machinery is not independent of speed and/or Reynolds number. This effect may not be small and variations up to 20% and more in the cavitation number, for the ratio of Reynolds numbers obtained in the present tests, have been observed on axisymmetric bodies.[5]

It can be seen in Fig. 5, then, that cavitation may well occur over a great part of the operating range of the pump unless large submergences are provided. From the standpoint of noise and damage cavitation even in a slight degree should be avoided.

Unfortunately, because of circuit limitations, it was not possible to extend the range of Figs. 4 and 5 to flow rates beyond the design point.

Similarity

Some of the difficulties in modeling cavitation inception have already been mentioned in the preceding paragraphs. In general, it may be said that inception cavitation numbers increase with increasing speeds and size, and that surface finish, etc., may also be important.[5] Once cavitation has

progressed to occupy a substantial zone, it is usually presumed that only the cavitation number K determines the flow behavior. In the case of two-dimensional shapes and bodies of revolution, such appears to be the case. In cavitation experiments on turbomachines the parameters employed (σ and S) bear a direct relation to the cavitation number K (see Appendix) so that these quantities should correctly provide cavitation similarity conditions. In case the Reynolds number is quite low and if the dissolved gas content is high or volatile fractions are present, as in petroleum mixtures, then one would expect deviations from this rule. However, these conditions do not usually occur in commercial practice and are beyond the scope of this work.

Photographs taken at two different speeds (1400 and 1700 rpm) on the test pump at the same value of σ, which was greater than that for Tenot's critical σ, show that the cavitation is indeed similar in shape and size (Fig. 7). Two operating points are shown, namely, Q_n and 38% Q_n.

In view of the above discussion and experimental evidence it is difficult to accept Tenot's hypothesis that cavitation scaling should follow the rule

$$\frac{\sigma_2 - \sigma_{crit}}{\sigma_1 - \sigma_{crit}} = \frac{H_1}{H_2} .$$

H_1 and H_2 are the heads of either two geometrically similar pumps or the same pump run at different speeds. The term σ_{crit} is presumably a value of σ which is the same for both pumps or conditions, and corresponds to a sharp break in the performance curve with increasing cavitation. However, in this work no such sharp break was observed (Fig. 5) in either the head or torque. Hence, unless unusual flow conditions obtain, i.e., low Reynolds numbers or volatile fractions present, any one of the parameters σ, K or S should characterize cavitation scaling when neither directly at the incipient conditions nor when unsteady, large scale pulsating cavitation occurs; this latter type being beyond the scope of the present work.

Photographic Study

In order to ascertain the location and magnitude of the zones of cavitation in the pump, two series of photographs were taken. The first series was taken over a range of flow rates somewhat before any noticeable change in performance occurred in the range of σ from about 5 to 6.5, and are shown in Fig. 8. The next series was taken about where the maximum rise in head

was observed under cavitating conditions and is shown in Fig. 9.

The first pictures in Fig. 8 show the edge of the pump blade just at the inception of cavitation and the vapor voids are first seen to occur at the extreme tip of the blade next to the wall (in all cases the radial tip clearance of the blade was about 0.010 in.). As the flow rate is progressively reduced, the cavitation is seen to increase only slightly at first, but at 38% design flow rate it increases somewhat more rapidly and the cavitating zone moves away from the tip and approaches the hub. The reasons for this latter behavior are not quite clear. The blade sections at the very low flow rates (about 30% Q_n) are badly stalled all along the span and large radial flows can occur. Moreover, the flow is not steady but pulsates erratically. With even lower suction pressures at these flow rates, large voids form and detach themselves rapidly and set up a very heavy vibration. Figure 9 shows the series at more reduced pressures, the sigma variation now being between 2 and 3.2 with the last photographs showing the violent cavitation attachment and separation.

The next series of photographs (Fig. 10) illustrates the progressive development of cavitation at the best efficiency point. In the last three of this series it is seen that the cavitation is "smeared out" over the wall or case and although it is difficult to see, cavitation also occurs along the remainder of the blade surface. The "striations" in the tip cavitation of these pictures strongly suggest the presence of a "tip clearance" flow, i.e., a flow through the tip clearance space, since their direction is more nearly perpendicular to the blade than in the direction of the shearing flow arising from the scraping motion of the blades as they move by the wall. Evidence of this phenomenon is more clearly shown in the next figure, which consists of a series of pictures taken at the best efficiency point but with a thinner polished blade of the same pump (Fig. 11). Cavitation inception is delayed on this blade until about $K = 0.64$ at which time minute cavities appear in the free stream nearly one-half blade chord downstream from the leading edge. More cavities appear until at a K of 0.50 they form a nearly continuous core which is attached to the leading edge and extends back about 1-1/2 chord lengths. No cavitation is seen to exist on the blade surface proper or within the tip clearance space itself. At a slightly lower pressure, the core becomes attached to

the blade and subsequently forms a more conventional picture of blade cavitation. In order to explain the appearance of the sharply-defined core of cavitation bubbles, it is presumed that the jet or sheet which flows through the tip clearance space interacts with the approaching relative velocity to form a *vortex sheet*. In turn the sheet can roll up to form a concentrated vortex. In the locally reduced pressure at the vortex center it would thus be possible for bubbles to form in the free stream or in the vicinity of the blade suction surface. Visually, this phenomenon seemed to depend upon the tip clearance, since the pump casing was out of round several thousandths and near inception the core was observed to be somewhat different in various circumferential locations.

It is seen that cavitation of the latter kind is produced in an entirely different way than the usual blade surface variety. Evidence of the same sort of vortex generation has also been shown in recent NACA literature[6] in the flow through stationary cascades of airfoils with tip clearance. It is reasonable to suppose that vortex cavitation will occur generally in axial flow machines and although no change in performance is observed for this condition, noise is produced which may be objectionable. The effects of blade design and flow parameters upon vortex cavitation were also beyond the scope of the present investigation.

CONCLUSIONS

Within the range of parameters investigated cavitation similarity was found to be governed by either the cavitation number K, σ or the suction specific speed S. Further cavitation tests should be made in the regions of large performance decrease to investigate the validity of the similarity laws for these conditions. A qualitative photographic investigation was conducted simultaneously to show the location and extent of cavitation on the blades. It was found that a relatively large amount of cavitation could exist and still cause only negligible changes, particularly in the head at a given flow rate and speed. Furthermore, cavitation inception was seen to occur at the blade tips and in some circumstances occurred first in the free stream away from the blade. Such cavitation is thought to be due to a vortex filament which arises from the interaction of the flow through the tip clearance space and the approaching free stream.

ACKNOWLEDGMENT

The project staff wishes to thank Mr. Paul Guinard, of "Pompes Guinard", for his indefatiguable efforts in accomplishing much of the experimental work reported by him.

REFERENCES

1. Tenot, M. A., "Phénomènes de la Cavitation", Bulletin de Mai-Juin 1934, Le Laboratoire de Mécanique de L'Ecole Nationale D'Arts et Metiers.

2. Osborne, W. C., Morelli, D. A., "Head and Flow Observations on a High Efficiency Free Centrifugal Pump Impeller", Trans. ASME, Oct. 1950.

3. Swanson, W. M., "Complete Characteristic Circle Diagrams for Turbomachinery", Trans. ASME, Vol. 75, No. 5, July 1953.

4. Wislicenus, G. F., "Fluid Mechanics of Turbomachinery", McGraw-Hill, 1947.

5. Kermeen, R. W., "Some Observations of Cavitation on Hemispherical Head Models", Hydrodynamics Laboratory Report No. E-35.1, June 1952, California Institute of Technology.

6. Hansen, A. G., Herzig, H. Z., Costello, G. R., "A Visualization Study of Secondary Flows in Cascades", NACA TN 2947.

APPENDIX

I. Notation

A - Circular area between case and hub

c - Absolute velocity

D - Diameter

g - Gravitational constant

H - Pump head - ft

K - Cavitation number = $p_1 - p_v / \frac{1}{2} \rho w_1^2$

N_s - Specific speed = RPM $\sqrt{gpm}/H^{3/4}$

NPSH - Net positive suction head = $p_1 - p_v/\rho g + c_1^2/2g$

p - Pressure

Q - Flow rate (cfs or gpm as noted)

Q_n - Flow rate at best efficiency

S - Suction specific speed = RPM $\sqrt{gpm}/(NPSH)^{3/4}$

T - Torque

u - Circumferential velocity

w - Relative velocity

ρ - Density (slugs/ft^3)

ψ - Head coefficient, $H/u_o^2/g$

φ - Flow rate coefficient, Q/Au_o, Q in cfs

τ - Torque coefficient, $\tau/\rho A r_o u_o^2$

σ - Cavitation parameter - NPSH/H (noncavitating)

η - Efficiency $= \varphi \psi / \tau$

Subscripts

a - Axial component

i - Inner or hub

Subscripts (cont'd)

o - Outer or tip

v - Vapor

1 - Conditions far upstream

II. Relation between the various cavitation parameters.

By means of the definitions in I above and Bernoulli's equation, the following relations can be obtained:

$$S = \frac{4840\ \varphi^{1/2}\sqrt{1 - \left[\frac{D_i}{D_o}\right]^2}}{(\psi\sigma)^{3/4}}$$

$$N_s = S(\sigma)^{3/4}$$

$$K = \frac{2\sigma\psi - \varphi^2}{1 + \varphi^2}$$

Hence it is seen that there is a direct connection between each of these parameters. Furthermore, since K is a constant for the blade row (neglecting Reynolds number and air or gaseous diffusion) it is clear that σ = constant is the condition for cavitation similarity as opposed to that of Ref. 1 (p. 6).

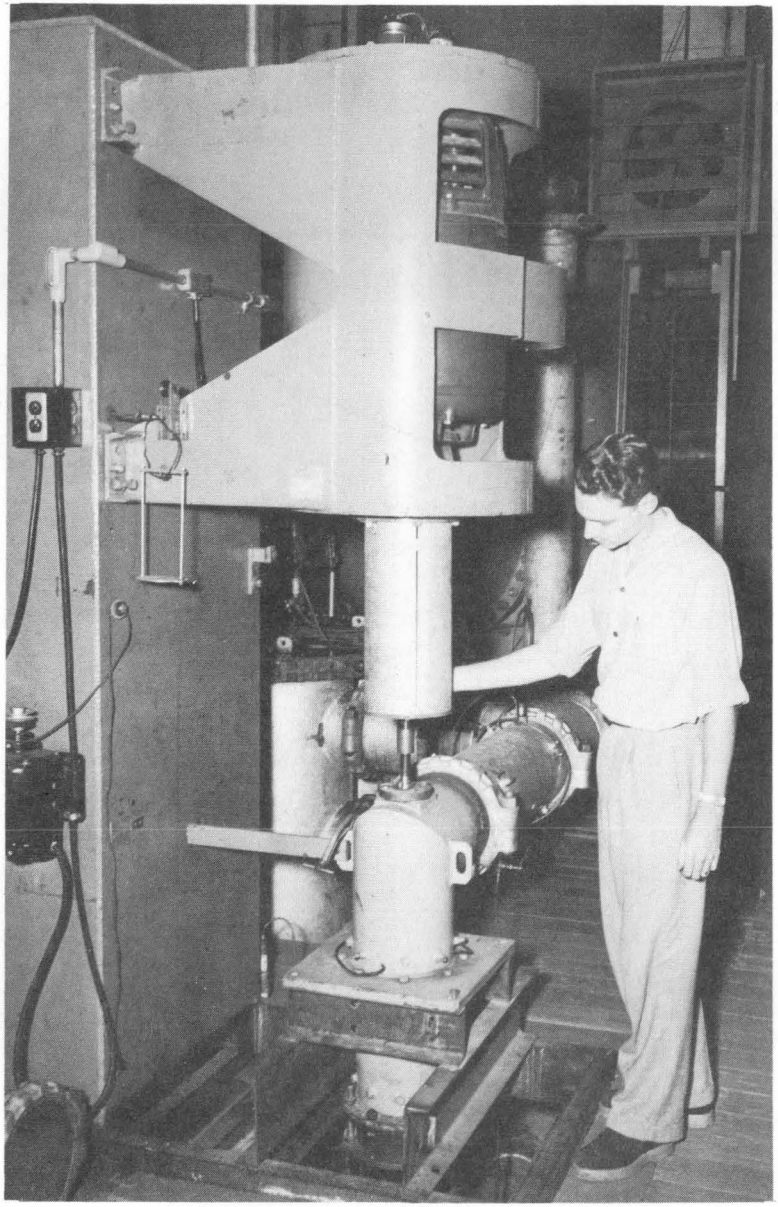

Fig. 1 - Installation showing test setup.

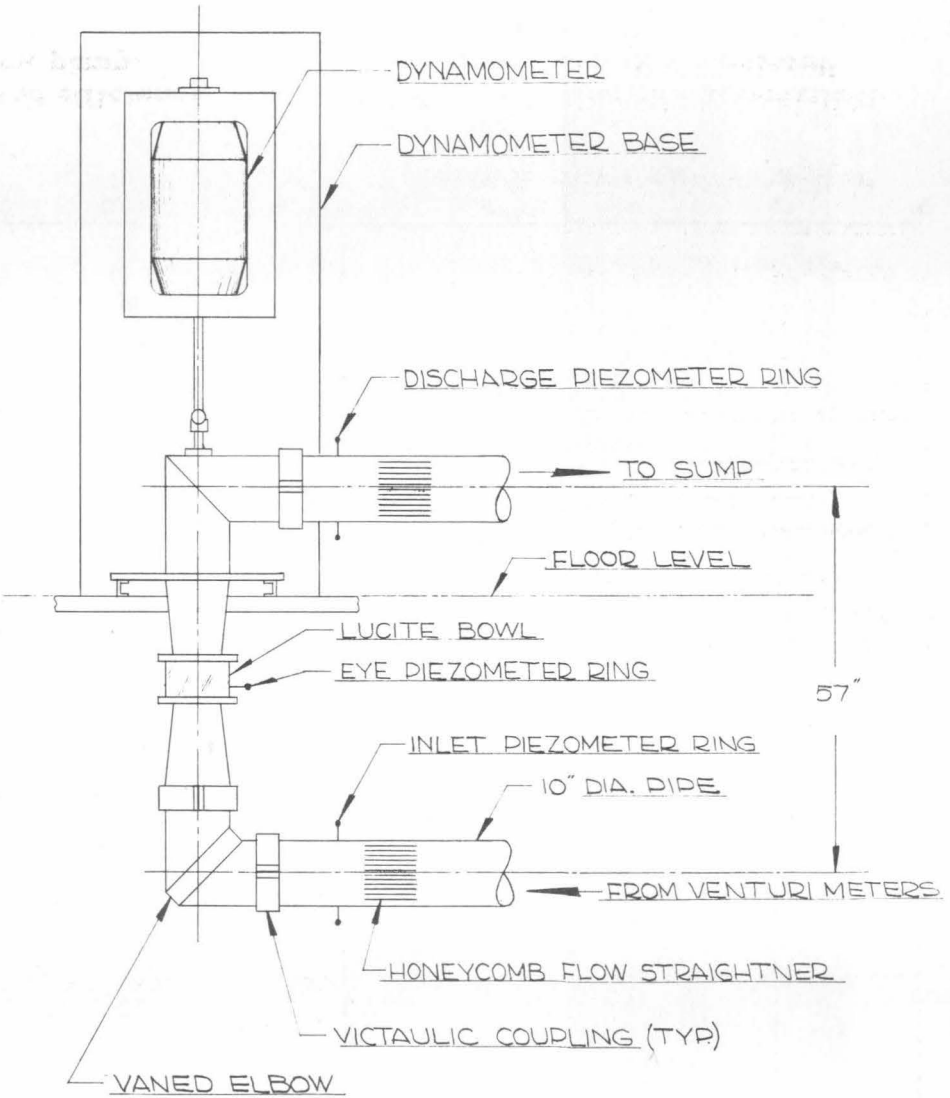

Fig. 2 - Schematic diagram of setup.

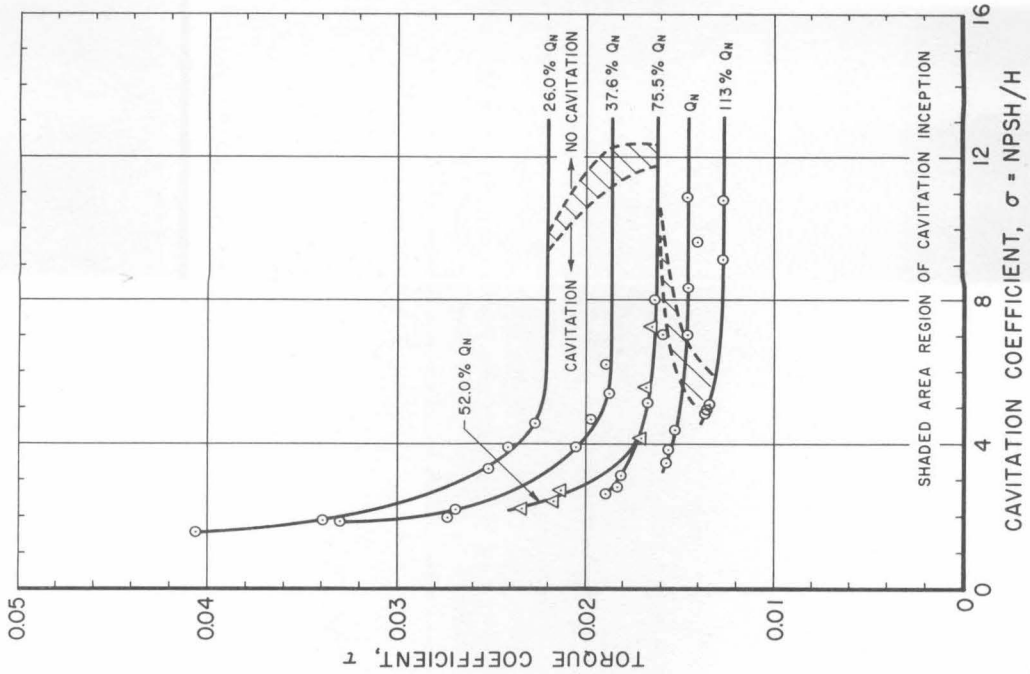

Fig. 4 - Cavitation characteristics. Torque vs. sigma at constant flow rate.

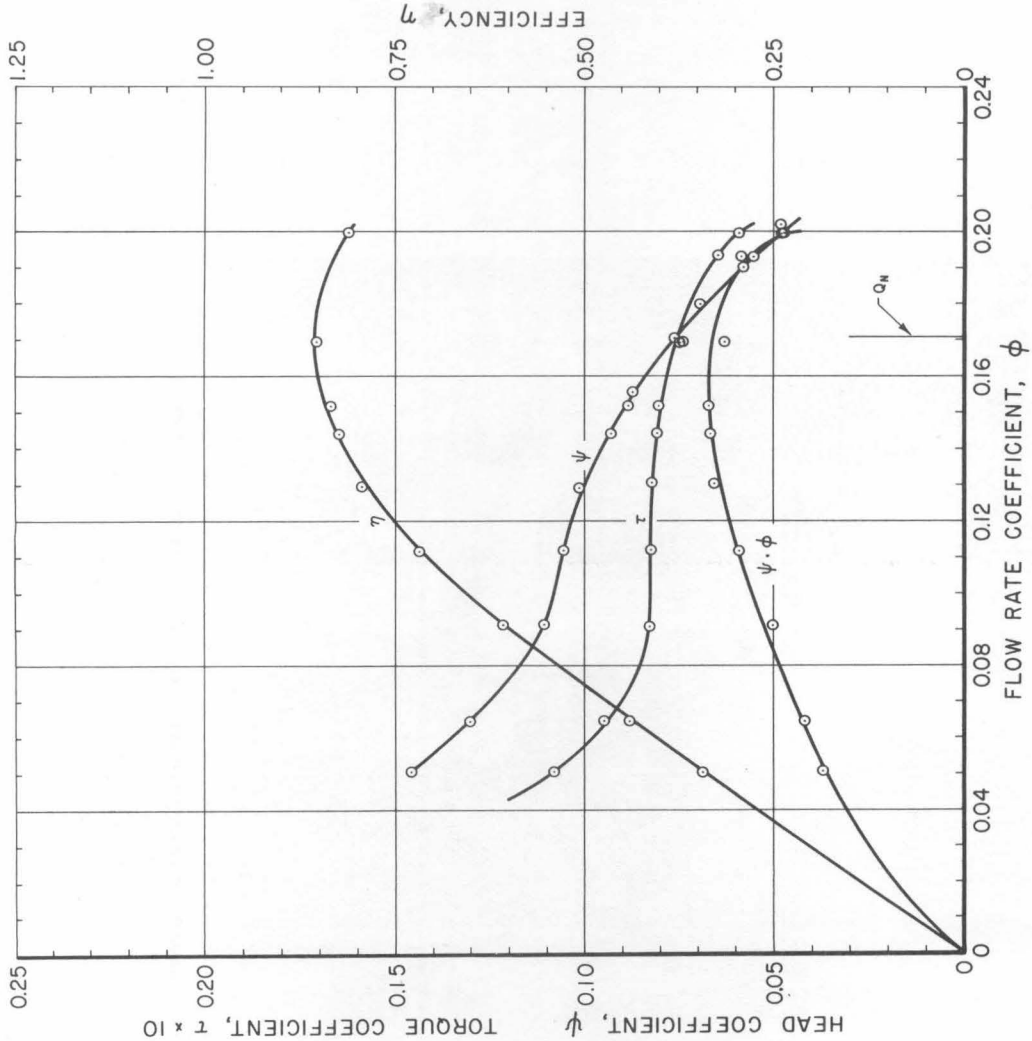

Fig. 3 - Characteristic curve showing head, torque and efficiency under noncavitating conditions for an 8" axial flow pump.

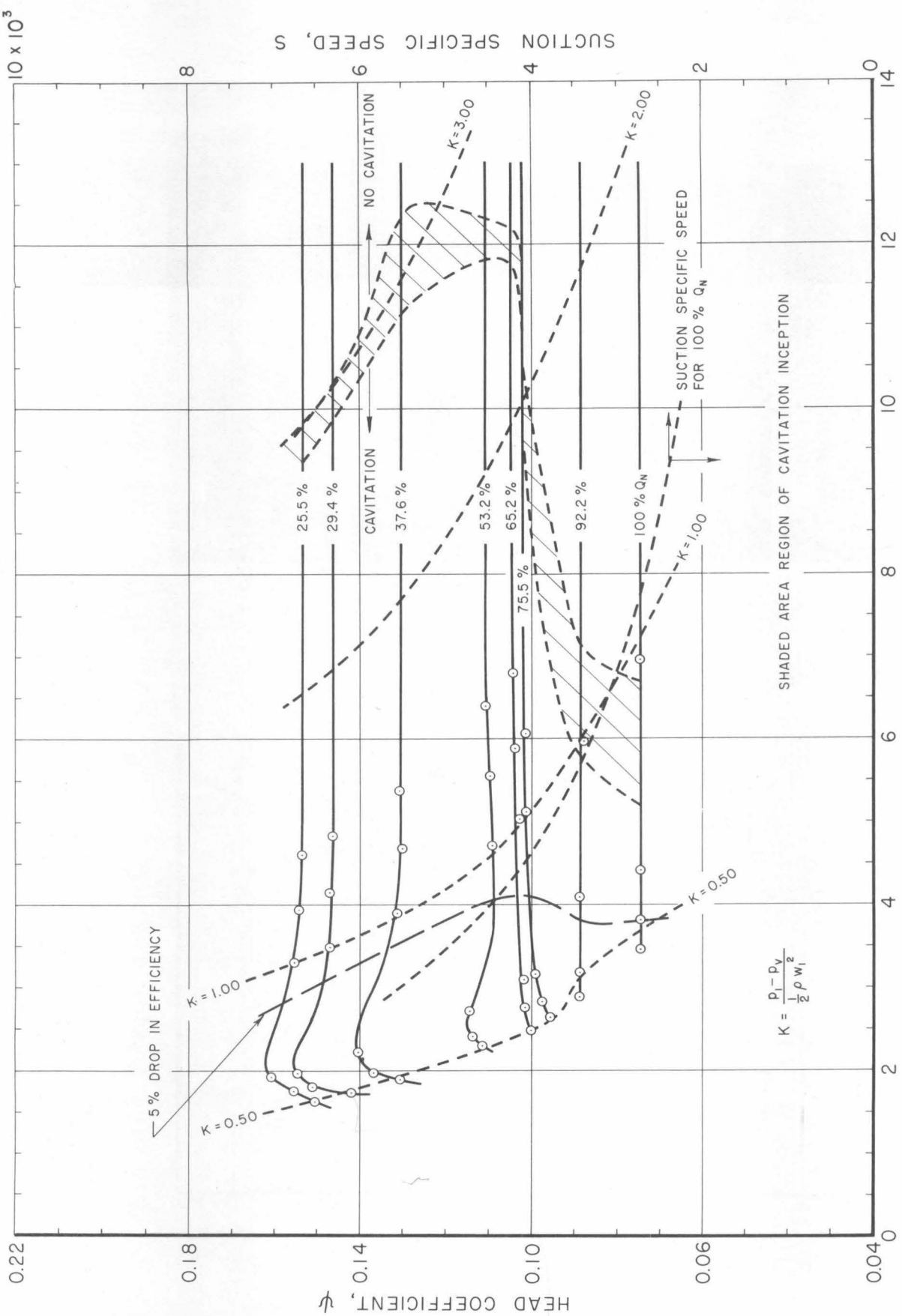

Fig. 5 - Cavitation characteristics. Head coefficient vs. cavitation parameter sigma for various flow rates.

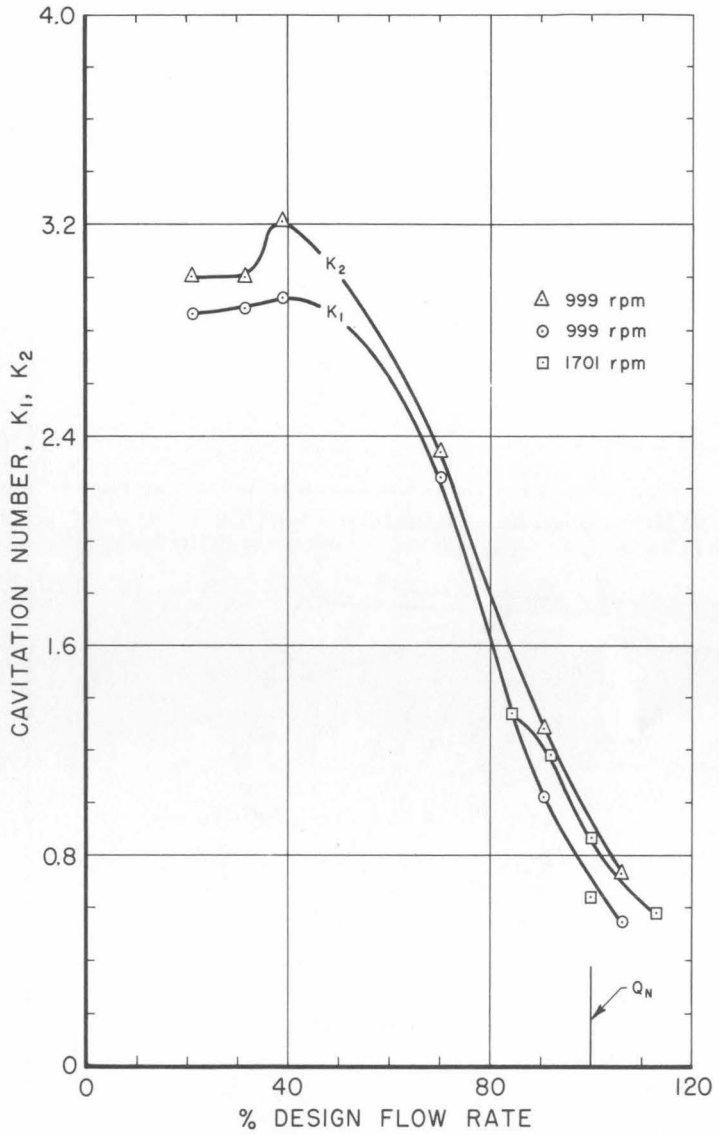

Fig. 6 - Cavitation characteristics. Incipient cavitation vs. percent design flow rate. The curve K_1 is for the first appearance of cavitation and curve K_2 for the disappearance of cavitation.

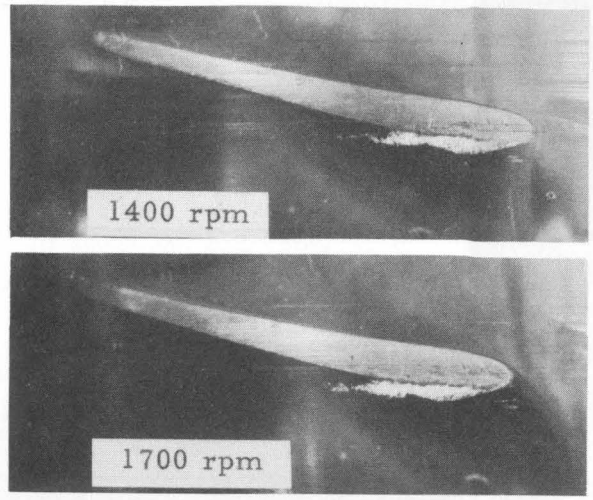

Design flow rate $\sigma = 4.6$

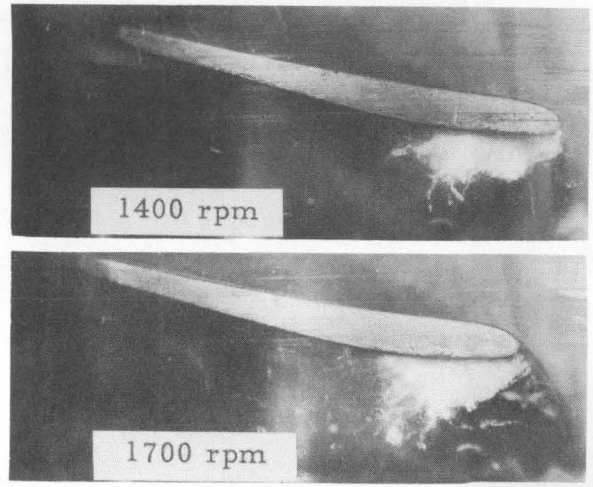

38% design flow rate $\sigma = 3.9$

Fig. 7 - Cavitation similarity at different speeds.

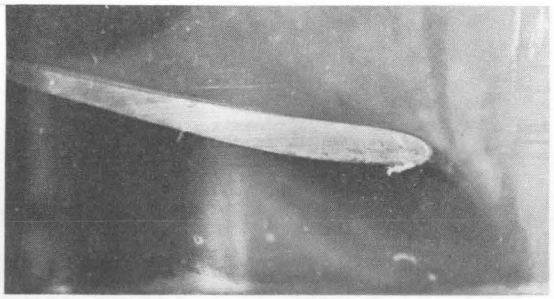

100% Q_n, σ = 6.45

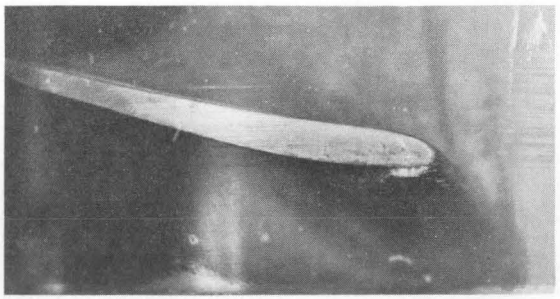

75.5% Q_n, σ = 6.45

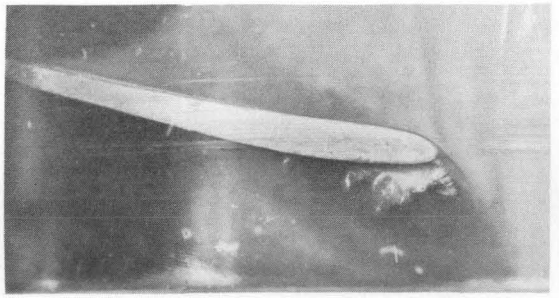

37.6% Q_n, σ = 6.1

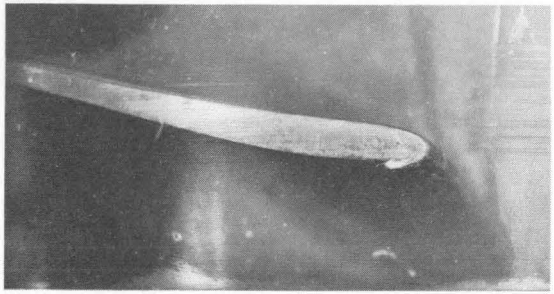

92.2% Q_n, σ = 6.45

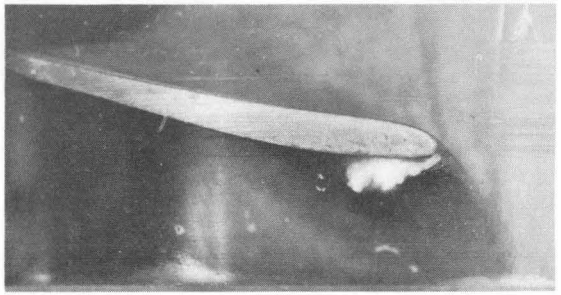

65.2% Q_n, σ = 6.45

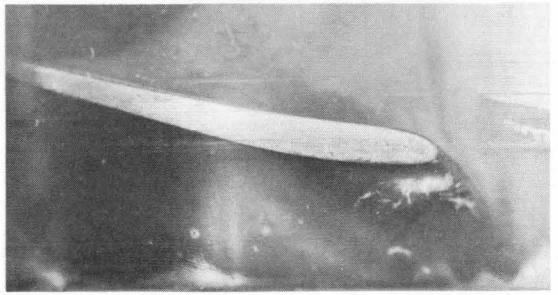

29.4% Q_n, σ = 5.25

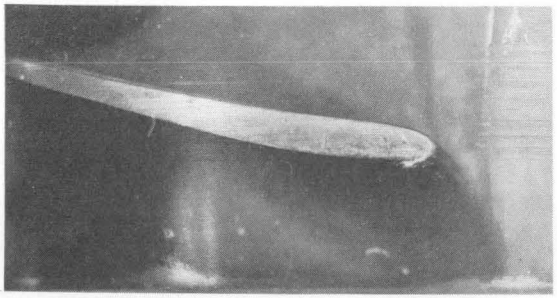

84.2% Q_n, σ = 6.45

53.2% Q_n, σ = 6.45

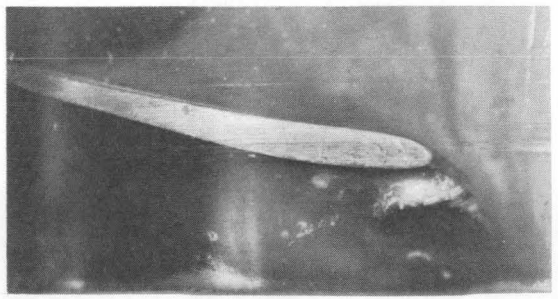

25.5% Q_n, σ = 4.75

Fig. 8 - Cavitation at various flow rates before any noticeable change in performance.

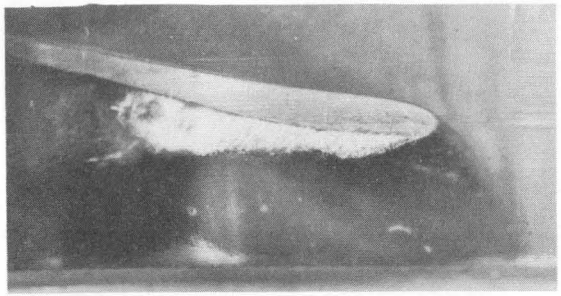

100% Q_n, σ = 3.2

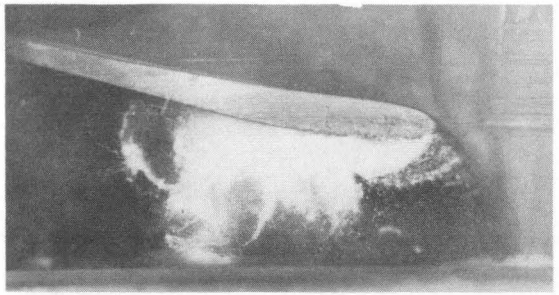

65.2% Q_n, σ = 2.85

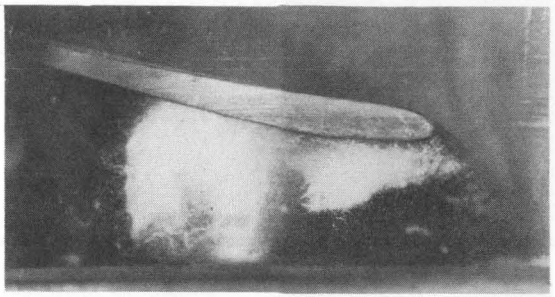

29.4% Q_n, σ = 2.15

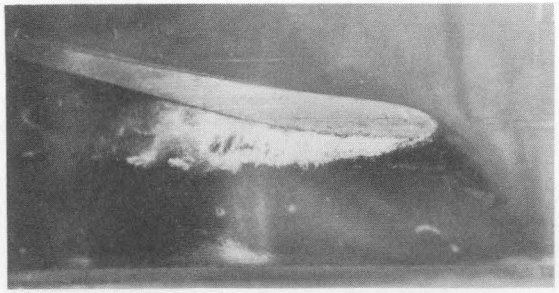

92.2% Q_n, σ = 3.15

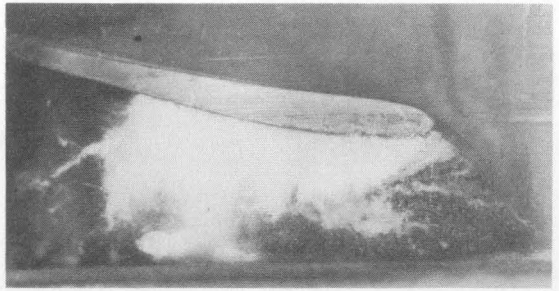

53.2% Q_n, σ = 2.65

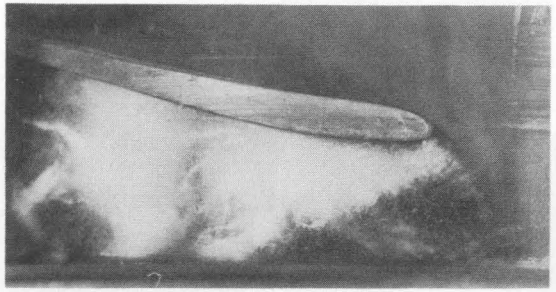

25.5% Q_n, σ = 2.05

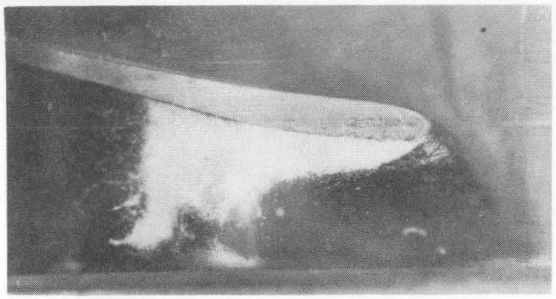

75.5% Q_n, σ = 3.00

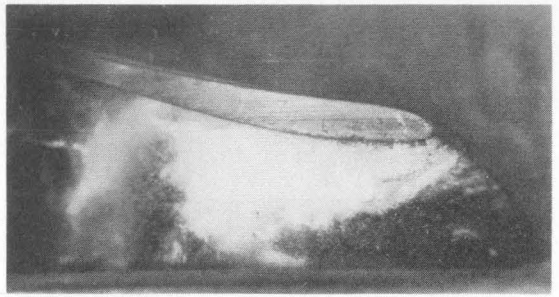

37.6% Q_n, σ = 2.40

Fig. 9 - Cavitation close to the point of maximum head increase in the ψ - σ plots.

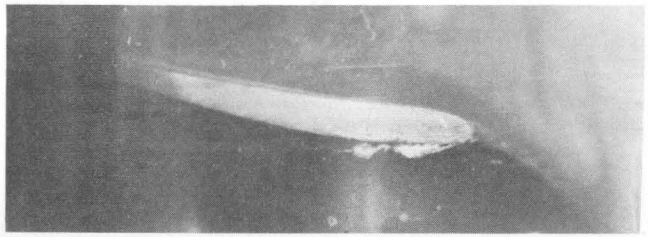

K = 0.73, σ = 5.27

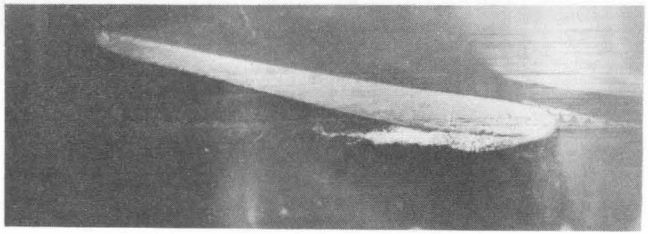

K = 0.62, σ = 4.54

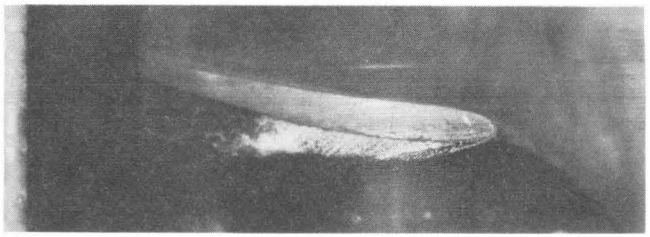

K = 0.50, σ = 3.70

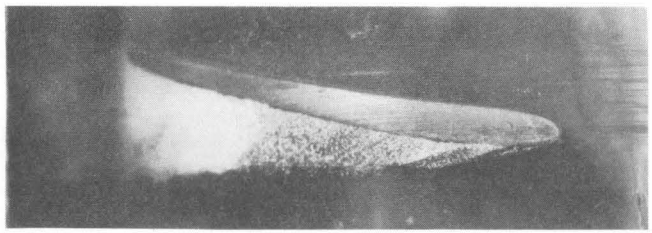

K = 0.42, σ = 3.12

Fig. 10 - Progressive development of cavitation with decreasing σ and K at the design point.

K = 0.64

K = 0.61

K = 0.58

K = 0.50

K = 0.45

Fig. 11 - Progressive development of cavitation on a thinner, polished blade of the same pump at the design flow rate.